Title: SOFT X-RAY DIAGNOSTICS FOR PULSED POWER MACHINES

Author(s): George C. Idzorek
William L. Coulter
Peter J. Walsh
Robert R. Montoya

Submitted to: 10th IEEE PULSED POWER CONFERENCE,
Albuquerque, NM
July 10-13, 1995

DISCLAIMER

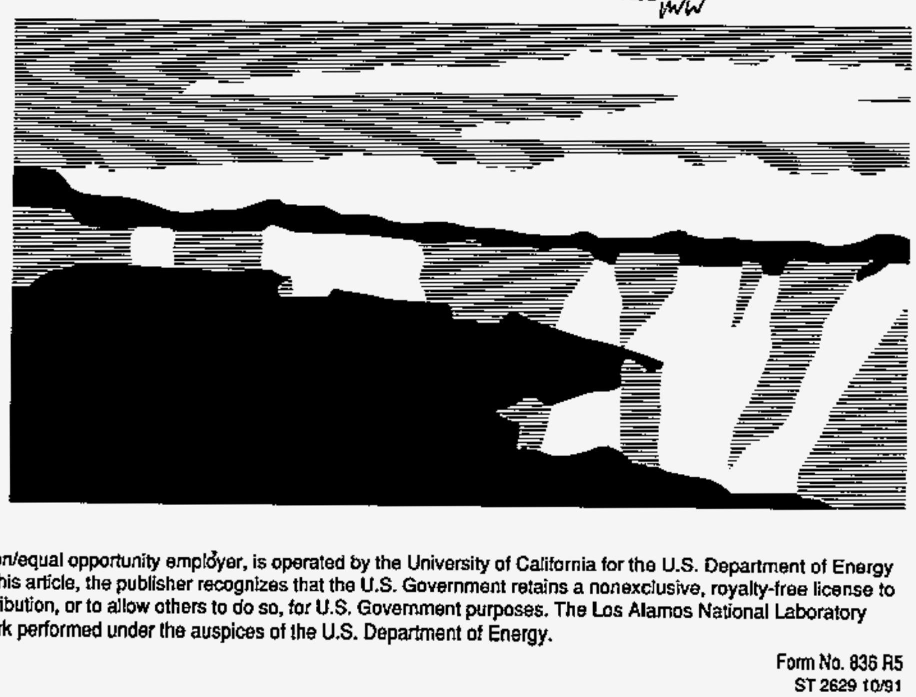

DISCLAIMER

Portions of this document may be illegible in electronic image products. Images are produced from the best available original document.

SOFT X-RAY DIAGNOSTICS FOR PULSED POWER MACHINES

G. C. Idzorek, W. L. Coulter, P. J. Walsh, R. R. Montoya
Los Alamos National Laboratory
Los Alamos, New Mexico, USA

A variety of soft x-ray diagnostics are being fielded on the Los Alamos National Laboratory Pegasus and Procyon pulsed power systems and also being fielded on joint US / Russian magnetized target fusion experiments known as MAGO (Magnitoye Obzhatiye).
We have designed a low-cost modular photoemissive detector designated the XRD-96 that uses commercial 1100 series aluminum for the photocathode.
In addition to photocathode detectors a number of designs using solid state silicon photodiodes have been designed and fielded.
We also present a soft x-ray time-integrated pinhole camera system that uses standard type TMAX-400 photographic film that obviates the need for expensive and no longer produced zero-overcoat soft x-ray emulsion film.
In a typical experiment the desired spectral energy cuts, signal intensity levels, and desired field of view will determine diagnostic geometry and x-ray filters selected. We have developed several computer codes to assist in the diagnostic design process and data deconvolution. Examples of the diagnostic design process and data analysis for a typical pulsed power experiment are presented.

Photoemissive detectors

Aluminum photocathode detectors have long been a standard for x-ray diagnostics. The relatively simple design principles, good sensitivity, high speed, and low cost make the aluminum cathode x-ray diode popular. The XRD-96 has an active area of 0.71 cm^2 , bias voltage of -1000 volts, linear range (as determined by space-charge limit) of 3 amperes, sub-nanosecond response time, up to four thin film x-ray filters, and typical operational noise of about 0.1 milliampere. In our XRD-96 detector standard commercial series 1100 and series 6061 aluminum stock is used for the cathode material based upon studies by Day[1] which showed quantum efficiency variation of about 10% between cathodes. Cathode surfaces are lathe cut using clean ethanol as a cutting lubricate and care is taken not to contaminate the photoemissive surface with oils. Photocathodes prepared this way quickly develop a stable Al_2O_3 layer that prevents changes in cathode quantum efficiency. In contrast Day notes that evaporated carbon and gold surfaces showed significant changes in quantum efficiency as they aged in air. Similar aging effects have observed by Saloman[2] on photocathodes stored under moderate vacuum. We are currently repeating the intercomparsion and aging studies of aluminum cathodes using our calibration facility at the Brookhaven National Laboratory, National Synchrotron Light Source. The Light Source provides a wider energy range and higher intensity than was available for Day's study. The calibration techniques we use at the Light Source are described in Idzorek and Hockaday[2].

Programmatic necessity required mass production of expendable detectors to characterize the implosion plasma generated in the Los Alamos National Laboratory pulsed power program. Additional budgetary constraints required the detectors must be produced at a much lower cost than the assemblies used previously. These requirements lead to the development of the XRD-96 detector shown in Fig.1. The XRD-96 consists of a vacuum leak checked type TNC bulkhead connector that serves as a vacuum feedthrough, cathode support, and attachment for x-ray filters. An aluminum barrel screwed onto the TNC serves as an electrical shield and filter support. Small venting holes are drilled in the side of the barrel to insure good vacuum is maintained inside the assembly. Selected x-ray filters and the detector anode mesh are mounted on washers which are dropped into the barrel followed by a stainless steel wave spring washer to prevent movement and insure good electrical contact. The washer stack and spring is held in place by a stainless steel snap ring which allows for easy last minute changes or repairs to the filters by merely removing the snap ring dumping out the filter stack, inserting the new stack and replacing the snap ring. Total parts cost (excluding filters) for the XRD-96 when mass produced is estimated at considerably less than $50 which is quite a savings over the $1000 parts cost of our previously used detectors.

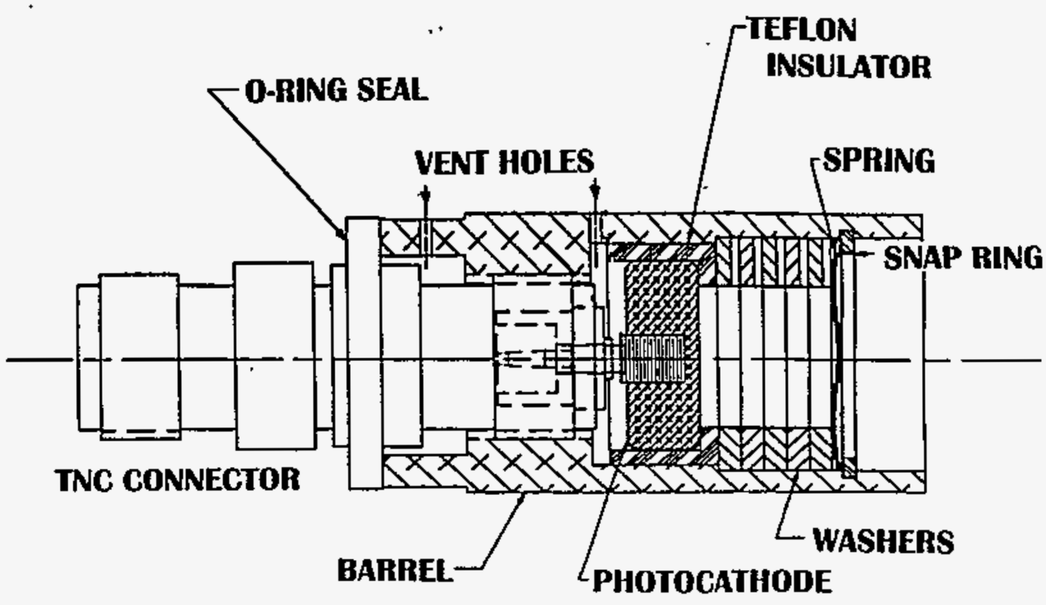

Fig. 1. The XRD-96 assembly

Photoionization detectors

Recent advances in fabrication technique have made the silicon photodiode detector attractive for pulsed power work. Unlike older silicon photodiodes the type HS-1 vacuum ultra-violet detectors made by International Radiation Detectors[4] are fabricated without a dead layer and a passivating layer only 60 angstroms thick. These features allow the new silicon photodiodes to be used at photon energies as low as 50 eV. Other advantages of silicon photodiodes include low bias voltage (0 - 50 volts), insensitivity to surface contamination, nominally flat response, 1/2 nanosecond rise time, ability to use very thin x-ray filters, and small size.

We are currently using our beamlines at the National Synchrotron Light Source to characterize the HS-1 detectors between 30 eV and 10 keV x-ray energy. In addition visible light characterization is being performed at the EG&G Las Vegas facility. When fully characterized the nominal flat detector responses will be replaced with calibrated values, source spectra deconvolved from the observed signals and cross checked with spectra deconvolved from XRD-96 detector signals. Our preliminary data show a visible light response of about 0.2 A/W peaking at 600 nm and falling off by a factor of 10 at 300 nm and 1000 nm. Measurements in the x-ray region are complicated by the small active area of the detector coupled with synchrotron x-ray beam non-uniformities. Preliminary data show a peak response near the nominal 0.27 A/W with structure appearing at the Si-k absorption edge. A drop in response is expected below the Si-k edge due to x-ray photons being transmitted through the 10-15 micron thick active layer into the substrate. Calibration efforts are continuing at the x-ray energies below the Si-k edge. We are also planning statistical studies of variations between individual HS-1 detectors.

Russian MAGO magnetized target fusion experiments required a windowless soft x-ray detector that could operate in a 10 torr hydrogen atmosphere which eliminated using photoemissive detectors due to their high vacuum requirement. Since the silicon diodes behave as solid ion chambers the gas fill has no effect upon their performance. A second MAGO requirement dictated that the gas volume of the detector be minimized so as to not affect the MAGO chamber performance. The third requirement was the detectors be insensitive to D-T fusion neutrons and gamma rays.

Five individual filtered HS-1 detectors were successfully fielded on the MAGO-II shot at Los Alamos on Oct. 20, 1994[12]. As anticipated the neutrons and gammas were undetectable and clean x-ray signals were measured. However, the symmetry of the MAGO-II system coupled with the failure of other diagnostics led to questions about the interpetation of the deconvolved spectral data. A new detector is being designed to answer these questions for the next shot.

An array of seven HS-1 detector chips is being fabricated into a compact 0.2" diameter array for use in upcoming MAGO-III experiments. By using different x-ray filters in front of each HS-1 detector a rough spectroscopic measurement can be obtained. Placing the detectors in a close coupled array insures the detectors are viewing the same location in the plasma without the need for a series of apertures to define the line of sight.

Photographic detectors

Radiography has long been used to provide images from photons above a few hundred eV. For softer x-rays the film overcoat prevents exposure of the film. Some special films without overcoats had been developed by Kodak for use in the ultra-violet however they are no longer manufactured in the United States and are difficult to handle. Another method to image soft x-rays is to first convert the x-rays to light with a scintillator and then use normal photographic film to record the image[5]. Because the scintillator response is flat the number of light photons is directly proportional to the number of incident x-ray photons. A severe problem with scintillator-film systems is that while a single x-ray photon can expose a silver grain in film it takes many visible photons appropriately spaced in time to accomplish the task[6]. This phenomenon is know as reciprocity failure and it makes calibration of the system difficult because one requires a calibration source that matches the experimental source being measured. However Rehnstrom[7] has observed that the reciprocity failure curve flattens out for sufficiently short exposure times. This allows the experimenter to obtain relative measurements of the image intensities.

A trick has been proposed to obtain absolute measurements by using the same bandpass filters on a camera as are used on arrays of XRD-96 filtered x-ray diodes. By using the XRD-96 signal to measure the absolute flux from the source one can use the pulsed power source being diagnosed as the calibration source for the film. By integrating the optical density, which is proportional to the log(exposure), of the image and setting it equal to the XRD-96 measured flux one obtains a calibration factor for the film.

Line-of-sight definition

It is necessary to constrain diagnostic detectors to insure that they are viewing only the desired part of the pulsed power experiment. Additionally care must be taken to insure low energy x-rays are not reflected off the internal pipe walls as the reflectivity for low angles of incidence can exceed 90% for soft x-rays[8]. A series of aperture plates can both define the field of view and eliminate reflections. We generally use three or four plates mounted on 1/4" drill rod for alignment. A single plate is chosen as the defining aperture plate and is located at an appropriate distance from the source to intercept the desired solid angle, hence determining the detector signal level. The other plates have aperture holes that are 1 mm larger than would be required if everything were perfectly aligned to allow for fabrication and assembly imperfections and insure the defining aperture defines the target field of view and solid angle intercepted by the detector. The detector location is determined by the desired source field of view, the defining aperture size and location, and the detector size related by the following formulas.

$$\textbf{Penumbra radius} = \left(\frac{L_1}{L_2}(r_d + r_a)\right) + r_a$$

if $r_d < r_a$

$$\textbf{Umbra radius} = \left(\frac{L_1}{L_2}(r_d - r_a)\right) - r_a$$

if $r_d > r_a$

$$\textbf{Umbra radius} = \left(\frac{L_1}{L_2}(r_a - r_d)\right) + r_a$$

Where:

L_1 = **source to defining aperture distance**
L_2 = **defining aperture to detector distance**
r_a = **defining aperture radius**
r_d = **detector radius**

As the source moves from the umbra into the penumbra the detector signal falls off approximately linearly yielding a trapezoidal shaped curve of signal level versus position. Because the source size and position are variable on most pulsed power experiments pinhole camera photographs are usually taken to verify the source falls completely within the detectors umbral field of view.

Spectral Deconvolution

The basic question addressed by our x-ray measurements is: what is the x-ray spectrum as a function of time. Unfortunately this cannot be answered precisely with a limited number of detectors. The signal output of each detector equals the integral of the detector response times the spectral intensity. Each detector response is generated from calibrations performed at the National Synchrotron Light Source augmented with extrapolations based upon past calibrations of similar detectors combined with filter responses calculated using optical constants databases.

Unfolding the spectral intensity involves solving the Fredholm integral equation, however, Fredholm problems are mathematically ill-posed (unstable solutions) so techniques must be used to smooth out the inversion process[9]. Further complicating the problem are the uncertainties in detector response data which typically are no better than about 10%. With imperfect data the best one can hope for is an approximate solution to the spectral unfold. In the computer code, UFO, Kissel[10] stabilizes the problem by supplying "auxiliary information" such as negative spectral intensity is forbidden and spectrum is smooth (i.e. no large spectral lines). Equally useful for approximate solutions is the LANL computer code SHAZAM.

The SHAZAM code operates by folding each detector response with a guess spectrum and then calculating a spectral bin adjustment factor from the sum of the detector sensitivities in that bin times the difference in calculated and observed signals for each detector. After each spectral bin is adjusted the spectrum is smoothed using a 3-point running average. The resulting spectrum becomes the new guess spectrum and the process is repeated until the calculated detector signals fall within desired error bars or an iteration limit is reached.

The final spectrum can then be integrated yielding a power output in terms of Watts / steradian. If one assumes a spherically symmetric source then the observed power output is π times the integral and remembering that the detector observes a circular cross section of the sphere then the output power must be multiplied by the ratio of the surface area of the sphere divided by the observed circle area. Therefore the total radiated power equals 4π times the integrated spectrum.

Energy output is obtained by plotting the calculated total radiated source output power as a function of time and then integrating the resulting curve. A quick method of estimating energy output is to assume that the detector with the widest photon bandwidth (generally an unfiltered XRD-96) has the same pulse shape as the output power. Setting the detector peak value equal to maximum power output and approximating the shape as a triangular waveform one obtains an approximate energy output that is the peak power times the full-width-half-max of the pulse shape. For our typical pulse shapes the quick method yields energy output within 15% of the more laborious calculation. Cross comparison between the XRD-96 calculated energy output and foil bolometer direct energy measurements are generally within 20% when the diagnostics are positioned to observe the same area of the source[11].

Acknowledgments

We wish to thank our machinist, Larry Rhodes, for his assistance in the fabrication of the prototype detectors, Los Alamos National Laboratory group J-7 for prototype engineering design, and EG&G Energy Measurements, Detector Engineering Division, Las Vegas, Nevada for the production of the XRD-96, vacuum line-of-sight assemblies, and silicon diode arrays, and EG&G Energy Measurements, Detector Engineering Division, Brookhaven National Laboratory, National Synchrotron Light Source for the calibration of the XRD-96 and silicon diode detectors. This work was performed under the auspices of the U. S. Department of Energy contract W-7405-ENG-36.

References

[1] R. H. Day, P. Lee, E. B. Salomon, D. J. Nagel, "X-ray Diodes for Laser Plasma Diagnostics," 1979 IEEE conf. on Plasma Science June 4-6 (1979)

[2] E. B. Saloman, "Typical photoefficiency between 20-250 eV windowless XUV photodiodes with tungsten and anodized aluminum photocathodes," Applied Optics, Vol. 17, No. 10, pp. 1489-1490 (1978)

[3] G. C. Idzorek, and R. G. Hockaday, "Calibration techniques for high-flux x-ray detectors," in X-Ray Detector Physics and Applications, Richard B. Hoover, Editor, Proc. SPIE 1736, pp. 149-158 (1993)

[4] K. W. Wenzel, C. K. Li, D. A. Pappas, R. J. Korde, "Soft X-Ray Photodiodes with 100% Quantum Efficiency," IEEE TRANSACTIONS ON NUCLEAR SCIENCE, Vol. 41, No. 4, pp. 979-983 (1994)

[5] R. A. Dudley, "Dosimetry with Photographic Emulsions," in Radiation Dosimetry Volume II second edition, F. H. Attix and W. C. Roesch, Editors, Academic Press, New York, pp. 325-387 (1966)

[6] J. F. Hamilton, "Reciprocity Failure and the Intermittency Effect," in The Theory of the Photographic Process, Fourth Edition, T. H. James, Editor, Macmillan Publishing Co, Inc., New York, pp. 133-145 (1977).

[7] A. Rehnstrom, "Reciprocity Failure of the Photographic Emulsion at Short Exposures," in Actes du Xeme Congres International de Cinematographie Ultra-Rapide, Association Nationale de la Recherche Technique, Paris, pp. 177-181, (1972)

[8] B. L. Henke, E. M. Gullikson, and J. C. Davis, "X-ray Interactions: Photoabsorption, Scattering, Transmission, and Reflection at E=50-30,000 eV, Z=1-92," Atomic and Nuclear Data Tables, Vol. 54, number 2, Academic Press (1993)

[9] X. Sun, D. L. Jaggard, "The inverse blackbody radiation problem: A regularization solution," J. Appl. Phys. Vol. 62 No. 11, pp. 4382-4386 (1987)

[10] L. Kissel, F. Biggs, T. Marking, "UFO (UnFold Operator) User Guide: Part 1- Overview and Brief Command Descriptions," Sandia Report #SAND82-0396, National Technical Information Service, US Department of Commerce (1991)

[11] H. Oona, D. L. Peterson, W. Anderson, J. Benage, G. Idzorek, M. L. Yapunich, C. Findley, J. Shlacter, J. H. Goforth, J. C. Cochrane, B. Anderson, "Instabilities in foil implosions and the effect on radiation output," This conference

[12] I. Lindemuth, R. Reinovsky, B. Anderson, J. Canada, R. Chrien, M. Christian, C. Ekdahl, C. Findley, J. Goforth, R. Haight, G. Idzorek, N. King, R. Kirkpatrick, G. Morgan, H. Oona, P. Rodriguez, P. Sheehey, J. Shlacter, R. Smith, G. Stradling, L. Veeser, B. Warthen, S. Younger, V. Chernyshev, V. Mokhov, N. Bidylo, A. Bukyo, A. Demin, V. Dolin, B. Egorychev, S. Garanin, V. Ivanov, V. Korchagin, O. Mikhailov, I. Morozov, S. Pak, E. Pavlovski, N. Seleznev, A. Skobelev, G. Volkov, V. Yakubov, " Joint US/Russian plasma formation experiments for Magnetized Target Fusion (MTF)," This conference